

- (1989); L. E. Kay, D. Marion, A. Bax, *J. Magn. Reson.* **84**, 72 (1989); E. R. P. Zuiderweg and S. W. Fesik, *Biochemistry* **28**, 2387 (1989); B. A. Messerle, G. Wider, G. Otting, C. Weber, K. Wüthrich, *J. Magn. Reson.* **85**, 608 (1989); M. Ikura, A. Bax, G. M. Clore, A. M. Gronenborn, *J. Am. Chem. Soc.* **112**, 9020 (1990); T. Frenkiel, C. Bauer, M. D. Carr, B. Birdsall, J. Feeney, *J. Magn. Reson.* **90**, 420 (1990).
36. D. Marion *et al.*, *Biochemistry* **29**, 6150 (1989).
37. G. M. Clore, A. Bax, A. M. Gronenborn, *J. Biomol. NMR*, in press.
38. P. C. Driscoll, G. M. Clore, D. Marion, P. T. Wingfield, A. M. Gronenborn, *Biochemistry* **29**, 3542 (1990); P. C. Driscoll, A. M. Gronenborn, P. T. Wingfield, G. M. Clore, *ibid.*, p. 4468.
39. M. Ikura, L. E. Kay, R. Tschudin, A. Bax, *J. Magn. Reson.* **86**, 204 (1990); E. R. P. Zuiderweg, L. P. McIntosh, F. W. Dahlquist, S. W. Fesik, *ibid.*, p. 210.
40. G. M. Clore, A. Bax, P. T. Wingfield, A. M. Gronenborn, *Biochemistry* **29**, 5671 (1990).
41. A. Bax *et al.*, *J. Magn. Reson.* **87**, 620 (1990); L. E. Kay and M. Ikura, A. Bax, *J. Am. Chem. Soc.* **112**, 888 (1990).
42. A. Bax, G. M. Clore, A. M. Gronenborn, *J. Magn. Reson.* **88**, 425 (1990).
43. G. M. Clore, A. Bax, P. C. Driscoll, P. T. Wingfield, A. M. Gronenborn, *Biochemistry* **29**, 8172 (1990).
44. L. E. Kay, G. M. Clore, A. Bax, A. M. Gronenborn, *Science* **249**, 411 (1990).
45. G. M. Clore, L. E. Kay, A. Bax, A. M. Gronenborn, *Biochemistry* **30**, 12 (1991).
46. E. R. P. Zuiderweg, A. M. Petros, S. W. Fesik, E. T. Olejniczak, *J. Am. Chem. Soc.* **113**, 370 (1991).
47. S. W. Fesik *et al.*, *ibid.* **112**, 886 (1990).
48. M. Ikura, L. E. Kay, A. Bax, *Biochemistry* **29**, 4659 (1990); L. E. Kay, M. Ikura, R. Tschudin, A. Bax, *J. Magn. Reson.* **89**, 496 (1990); L. E. Kay, M. Ikura, A. Bax, *ibid.* **91**, 84 (1991); M. Ikura and A. Bax, *J. Biomol. NMR*, in press; R. Powers, A. M. Gronenborn, A. Bax, *J. Magn. Reson.*, in press.
49. G. M. Clore, P. C. Driscoll, P. T. Wingfield, A. M. Gronenborn, *J. Mol. Biol.* **214**, 811 (1990).
50. M. Karplus, *J. Am. Chem. Soc.* **85**, 2870 (1963); A. DeMarco, M. Llina, K. Wüthrich, *Biopolymers* **17**, 617 (1978); A. Pardi, M. Billeter, K. Wüthrich, *J. Mol. Biol.* **180**, 741 (1984).
51. L. E. Kay and A. Bax, *J. Magn. Reson.* **86**, 110 (1990); A. M. Gronenborn, A. Bax, P. T. Wingfield, G. M. Clore, *FEBS Lett.* **243**, 93 (1989); J. D. Forman-Kay, A. M. Gronenborn, L. E. Kay, P. T. Wingfield, G. M. Clore, *Biochemistry* **29**, 1566 (1990).
52. L. Mueller, *J. Magn. Reson.* **72**, 191 (1987); A. Bax and L. E. Lerner, *ibid.* **79**, 429 (1988); D. Marion and A. Bax, *ibid.* **80**, 528 (1988).
53. We thank our many colleagues, past and present, who have contributed to the work carried out in our laboratory. Above all others, we thank A. Bax, with whom we have shared numerous stimulating discussions, fruitful experiments, and a continuous and most enjoyable collaboration in the best of scientific spirits. In addition, we thank W. Eaton and A. Szabo for many constructive and helpful comments during the preparation of this manuscript. The work in the authors' laboratory was supported in part by the AIDS Targeted Anti-Viral Program of the Office of the Director of the National Institutes of Health.

Research Article

Asteroid 1986 DA: Radar Evidence for a Metallic Composition

S. J. OSTRO, D. B. CAMPBELL, J. F. CHANDLER, A. A. HINE, R. S. HUDSON,
K. D. ROSEMA, I. I. SHAPIRO

Echoes from the near-Earth object 1986 DA show it to be significantly more reflective than other radar-detected asteroids. This result supports the hypothesis that 1986 DA is a piece of NiFe metal derived from the interior of a much larger object that melted, differentiated, cooled, and subsequently was disrupted in a catastrophic collision. This 2-kilometer asteroid, which appears smooth at centimeter to meter scales but extremely irregular at 10- to 100-meter scales, might be (or have been a part of) the parent body of some iron meteorites.

NEAR-EARTH ASTEROIDS, LIKE METEORITES, ARE THOUGHT to come primarily from mainbelt asteroids (1, 2). The relations among meteorites, near-Earth asteroids (NEAs), mainbelt asteroids (MBAs), and comets are central to our understanding of conditions in the primitive solar nebula, planetary

formation, the collisional evolution of the asteroid belt, and the delivery of small bodies into Earth-crossing orbits. As compositions of asteroids bear directly on these issues, much astronomical effort is devoted to obtaining and interpreting information about asteroid mineralogy. Many NEAs and MBAs have been classified on the basis of their photometric colors and albedos. Visible-infrared (VIS-IR) reflectance spectra have established important mineralogical characteristics that limit the set of plausible meteorite analogs for the most populous classes (3-7). For example, C asteroids contain hydrated silicates, carbon, organics, and opaques and are analogous to CII and CM2 carbonaceous chondrites. The S asteroids contain pyroxene, olivine, and NiFe metal, and probably correspond to stony iron meteorites or ordinary chondrites or both. The M asteroids contain NiFe metal or assemblages of enstatite and NiFe metal or a combination of both, and probably correspond to iron meteorites or enstatite chondrites or both.

Iron and stony iron meteorites are igneous assemblages derived from differentiated parent bodies, whereas chondrites are relatively primitive, undifferentiated assemblages, so the different candidate meteoritic analogs to the M and S classes have disparate cosmogonic implications. Radar observations can probe asteroid-meteorite relations because metal concentration influences radar reflectivity dramatically and iron and stony iron meteorites are much more metallic than chondrites. Only two M NEAs, 1986 DA and 3554 Amun (1986 EB), have been identified (8, 9). We report radar observations of 1986 DA that constrain this object's physical properties, and we argue that it is mineralogically similar to iron meteorites.

S. J. Ostro and K. D. Rosema are at the Jet Propulsion Laboratory, California Institute of Technology, Pasadena, CA 91109. D. B. Campbell is at the National Astronomy and Ionosphere Center, Cornell University, Ithaca, NY 14853. J. F. Chandler and I. I. Shapiro are at the Harvard-Smithsonian Center for Astrophysics, Cambridge, MA 02138. A. A. Hine is at the National Astronomy and Ionosphere Center, Box 995, Arecibo, PR 00613. R. S. Hudson is in the Electrical and Computer Engineering Department, Washington State University, Pullman, WA 99164.

Table 1. The orbit of asteroid 1986 DA. These osculating orbital elements are based on analysis of the combined radar and optical astrometric data, and are referred to the mean ecliptic and equinox of B1950.0. Our estimate of standard error in each of these elements is about 1 in the last decimal place shown, based in part on a comparison of solutions using different sets of planetary ephemerides. The mean motion and period are based on the orbit solution and averaged over the 50-year span starting in 1986.

Epoch: 1986 Mar. 31.0 TDT = JD 2446520.5	
Semimajor axis, a	2.81164 AU
Eccentricity, e	0.58538
Inclination, i	4.2958°
Longitude of ascending node, Ω	64.5355°
Argument of perihelion, ω	126.7040°
Mean anomaly, M	358.4117°
Mean motion, n	0.2085° per day
Period	4.728 year

Observations. 1986 DA was discovered by M. Kizawa (10) at Shizuoka, Japan, on 16 February 1986. Two months later, we observed it with the Arecibo Observatory's 2380-MHz (13-cm) radar. Our experimental techniques were essentially the same as those used in other asteroid radar investigations (11–14). During 18 to 20 April we did “cw” runs, in which we transmitted an unmodulated, continuous wave and measured the distribution of echo power as a function of frequency. The resultant echo spectra can be thought of as one-dimensional images, or brightness scans, across 1986 DA through a slit parallel to the asteroid's apparent spin vector. We devoted 21 April to “ranging” runs, in which a time-coded wave form was transmitted and the distribution of echo power in time delay and Doppler frequency was measured. During 18 to 21 April the asteroid's distance, right ascension, and declination changed little, from (0.207 AU, 12.0 h, 18°) to (0.210 AU, 12.2 h, 16°). Each day's observing window was 1.3 h to 4.1 h UTC (coordinated universal time).

Each run involved transmission for 3.5 min (the round-trip light time to the asteroid) followed by reception of echoes for a similar period. The transmission was circularly polarized, and echoes were received simultaneously in the same circular polarization as transmitted (the SC sense) and in the opposite (OC) sense. 1986 DA's apparent radial motion introduced a continuously changing Doppler shift into the echoes, but we avoided spectral smear by tuning the receiver according to an ephemeris based on an orbit determined from optical observations of the asteroid.

Optical light curves obtained within a few weeks of the radar observations indicate a value for the apparent rotation period, P , within 0.1 hour of 3.5 hours (15). Comparisons of echo spectra from 18 to 21 April support that value. Our observations, which spanned ~2.5 hours on each date, yielded a total of 65 useful runs (57 cw plus 8 ranging), that individually span 6° of rotation phase and collectively provide thorough phase coverage (Fig. 1).

Orbit determination. We derived an orbit for 1986 DA and searched for future close approaches using the radar delay–Doppler results in combination with all of the available optical astrometric data (Table 1). During the apparition in 1986, the asteroid approached Earth to within 0.21 AU, which is nearly as close as possible in the present state of its orbital evolution because the asteroid's perihelion roughly coincided with its opposition. A similar approach will occur in 2038, but no other approaches closer than 0.6 AU will occur until then. In that the asteroid's orbit crosses that of Mars, extremely close approaches are possible between those two bodies, but none closer than 0.2 AU will occur in the next century.

Perhaps the most interesting feature of 1986 DA's present orbit is that its period is within 1 percent of a 5:2 resonance with Jupiter, which is comparable to the closeness of Jupiter's period to the 5:2 resonance with Saturn. Hahn *et al.* (16) demonstrated that such asteroid orbits are chaotically unstable on time scales of 10^4 to 10^5

years. Over longer time scales, 1986 DA's orbit might intersect the orbit of Earth as a consequence of secular perturbations by the planets, and for this reason 1986 DA is referred to as an Earth-crossing asteroid (17).

Shape and surface structure. The bandwidth B of an asteroid's instantaneous echo power spectrum is related to the breadth D_{sil} (measured normal to the line of sight) of the asteroid's pole-on silhouette by $B = (4\pi D_{sil} \cos \delta)/(\lambda P)$, where P is the apparent rotation period, δ is the angle between the asteroid's equatorial plane and the radar line of sight, and λ is the radar wavelength. Measurements of echo edge frequencies as functions of rotation phase can be used to estimate the convex envelope, or “hull,” of the pole-on silhouette as well as the offset f_o of the frequency of hypothetical echoes from the asteroid's center of mass (COM) from the ephemeris prediction. (The hull can be thought of as the shape of a rubber band stretched around that silhouette.) The COM's location in projection within the hull and the Fourier series expansion of the hull's shape depend on f_o , which is treated as a free parameter in the least-squares estimation (18). Application of procedures described in those references to our echo spectra yielded the hull estimate in Fig. 1A. The apparently modest elongation of the hull, 1.4 ± 0.2 , is consistent with the ratio of brightness extrema in optical light curves. However, as illustrated in Fig. 1B, the data's noise level precludes high-precision estimation of the hull's detailed shape, that is, the curvature of the hull's approaching limb as a function of rotation phase.

The OC and SC weighted sums of our cw echo spectra are shown in Fig. 2A. 1986 DA's SC/OC ratio ($\mu_c = 0.09 \pm 0.02$) indicates that the echoes are almost entirely due to single reflections from surface elements that are smooth at scales of centimeters to meters. However, pronounced variations in the OC spectral signature as a function of rotation phase (Fig. 2B) indicate that the asteroid's surface possesses extreme structural complexity at 10- to 100-m scales. For example, bimodal spectra occur within two phase intervals roughly one half of a rotation apart, which is the signature

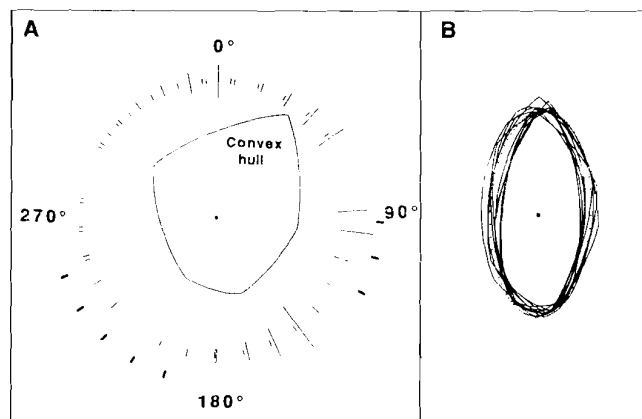
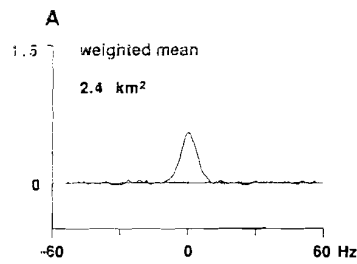
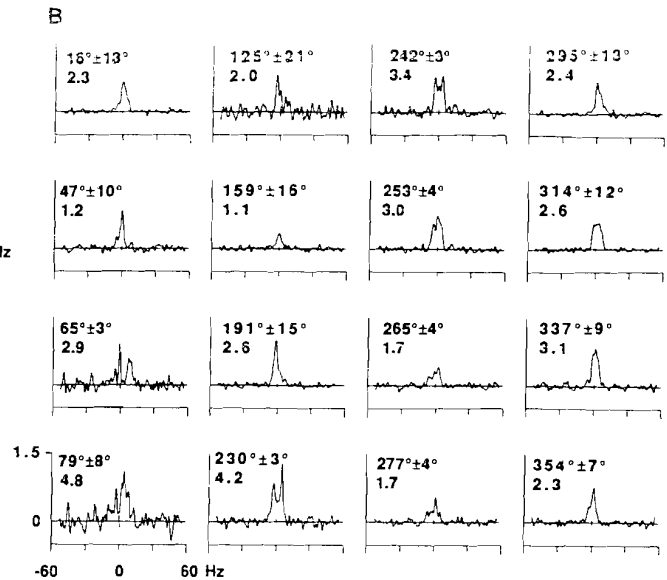


Fig. 1. Rotation phases of 1986 DA observations and the estimate of its asteroid's hull. (A) Phases of cw and ranging runs (light and dark radial line segments), based on $P = 3.50$ h and phase origin at 1986 April 21.75 UT. The line segment for any given run gives the radar's orientation with respect to the hull. Lengths of lines are proportional to background noise level and their variation reflects the zenith-angle dependence of the Arecibo telescope's sensitivity. The convex hull can be thought of as the shape of a rubber band stretched around the asteroid's pole-on silhouette. The central dot is the asteroid's projected center of mass. (B) Simulations designed to explore the accuracy of estimates of 1986 DA's hull. The dotted profile is the true hull of an ellipsoidal (convex) model asteroid and the solid curves are estimates derived from simulated echo spectra contaminated with noise. Uncertainty in the estimate of 1986 DA's hull is indicated graphically by the dispersion of the solid curves about the dotted ellipse, as in (18).

Fig. 2. (A) Weighted sums of cw echo spectra obtained for 1986 DA in the OC and SC polarizations (solid and dotted curves, respectively). Echo power, in square kilometers of radar cross section per 2-Hz frequency bin, is plotted versus frequency; 0 Hz corresponds to hypothetical echoes from the asteroid's center of mass. The vertical bar at the origin indicates ± 1 standard deviation of the receiver noise.



(B) Weighted sums of OC spectra in 16 independent groups that cover different intervals of rotation phase. Labels give weighted mean phase, approximate phase range, and OC radar cross section in square kilometers.



expected for a target with a bifurcated mass distribution (12). The remaining spectra are unimodal; some are fairly symmetrical and centered within the band occupied by the echoes in Fig. 2A, whereas others occupy primarily the left or right side of that band. The eight delay-Doppler images (Fig. 3) show similarly complex behavior, with the locations of the peaks of the echo jumping around in range as well as frequency. The overall pattern in Figs. 2 and 3 indicates that 1986 DA's shape is extremely irregular, highly nonconvex, and possibly bifurcated.

Size and radar reflectivity. How big is 1986 DA? This question is important because the asteroid's composition is constrained by the radar albedo, $\hat{\sigma}_{oc} = \sigma_{oc}/A_{proj}$, with σ_{oc} the object's radar cross section and A_{proj} its apparent projected area. The object's dimensions are bounded by the delay-Doppler extent of its radar echoes as follows. First, the range extent of echoes in the eight-run sum (Fig. 3) is 1.8 ± 0.6 km. The furthest portions of the asteroid return no echoes because they face away from the radar, so the asteroid's full range extent is larger than that seen by the radar by an amount that depends on the asteroid's shape, scattering properties, and orientation. Second, the hull estimation yields values of $[(1.4, 1.6, 1.9) \pm 0.3]$ km/(cos δ) for the minimum, mean, and maximum breadths of the asteroid's pole-on silhouette. The hull's area is (1.9 ± 0.7) km²/(cos² δ), that is, the hull's areal diameter is $D = (4A_{proj}/\pi)^{1/2} = (1.5 \pm 0.3)$ km/(cos δ).

The radar view was probably at least several tens of degrees from pole-on because the range distribution of echo power (Fig. 3) is a rapidly changing function of rotation phase. In view of the hull's modest elongation, the high amplitudes of optical light curves (15) taken at solar phase angles $\sim 32^\circ$ during the week of the radar observations also argue for an orientation at least several tens of degrees from pole-on (19). Accordingly, we adopt 60° as an upper bound on δ . The corresponding upper bound on the hull's areal diameter is 3.0 km. 1986 DA's pole-on silhouette presumably contains concavities, so its areal diameter presumably is smaller than the hull's.

Might the radar view have been nearly equatorial ($\delta \sim 0^\circ$)? If so, then the hull's range extent during the three ranging experiments centered on phase 104° would have been 1.4 ± 0.3 km, which is less than the range extent of echoes observed in those runs (Fig. 3). However, given the coarseness of our range resolution, an equatorial view cannot be ruled out.

Apart from the radar results, the only other constraint on 1986 DA's size is the areal diameter estimate, $D = 2.3 \pm 0.1$ km, obtained by Tedesco and Gradie (8) from disc-integrated, 0.36- to 20- μ m observations made during the 1986 apparition. The quoted error reflects only the measurements' precision; uncertainties involving the nature of the thermophysical model are at least several times greater (20).

Given the available information, we feel that a "safe" interval estimate of 1986 DA's areal diameter is $1.7 \leq D \leq 2.9$ km. Our

estimate of the asteroid's radar cross section is $\sigma_{oc} = 2.4$ km². Whereas the absolute calibration of the Arecibo telescope's sensitivity is known to ~ 35 percent, relative uncertainties applicable to the target-to-target comparisons of interest here are ~ 15 percent; thus our interval estimate for 1986 DA's radar albedo is $0.31 \leq \hat{\sigma}_{oc} \leq 1.2$. However, in order to consider the compositional implications of 1986 DA's radar albedo, we find it desirable to compare albedos of many asteroids whose sizes are currently constrained better from thermal radiometry than from radar. Therefore, we rely exclusively on albedos based on radiometrically determined sizes (for example, 0.58 for 1986 DA) to try to minimize systematic errors in the relative albedo estimates discussed below.

Metal abundance and meteoritic association. The estimate of 1986 DA's radar albedo is much larger than those of other radar-detected asteroids (Table 2 and Fig. 4). Let us interpret this result in the context of the electrical properties of plausible meteorite analogs to those asteroids in order to constrain 1986 DA's mineralogy. Recall that analogs to M asteroids like 1986 DA are irons and enstatite (E) chondrites, whereas analogs to S asteroids are stony irons and ordinary chondrites (Table 3). The Fresnel power-reflection coefficient at normal incidence, R , increases with metal concentration so that irons and stony irons are more reflective than chondrites, and solid meteorites are more reflective than powdered meteorites (Fig. 4C). Thus an asteroid covered with a substantial "regolith" of porous, unconsolidated, fragmental debris would be less reflective than if its surface were exposed bedrock. Models of regolith formation (21) predict that 1- to 10-km-diameter "weak" asteroids, possessing internal strength comparable to that of loose regolith, develop regoliths centimeters to meters in thickness, whereas asteroids as strong as basalt maintain much thinner coatings. The radar absorption length in dry, powdered rocks is about ten wavelengths (22), so a regolith more than 1 m thick would "hide" underlying bedrock from the radar. A much thinner regolith can act similarly if it has a density gradient that matches the bedrock's impedance to that of free space, or if it has stratifications containing lossy layers that create certain resonance effects (23).

For targets with low μ_c , the albedo can be thought of as the product of R and a gain factor G that depends on the target's shape at scales greater than or equal to λ . Asteroids as large as the radar-detected mainbelt objects ($D \geq 100$ km) are expected to be covered with regoliths more than 15 m thick (21). In light of

expectations about such objects' shapes and surface-slope distributions, G is probably within a few tens of percent of unity (24), so $\hat{\sigma}_{oc}$ is a reasonable first approximation to R . For dry, powdered mixtures of meteoritic minerals, R depends almost linearly on bulk density. Hence R for any given mineral assemblage is a nearly linear function of porosity (Fig. 4C). For example, the highest MBA albedo, for the M asteroid 16 Psyche, is consistent with a metallic regolith having a porosity (~ 0.55) typical of lunar soil, whereas the M asteroid 97 Klotho's albedo is compatible with either a rather low-porosity,

E-chondritic regolith or a rather high-porosity, metallic regolith.

For the smaller, more irregularly shaped NEAs, G might be a strong function of orientation and cause radar cross sections to vary much more dramatically than A_{proj} as the object rotates. Severe variation in σ_{oc} with rotation phase is in fact seen for 1986 DA (Fig. 2B). NEA albedos derived from observations with thorough rotation-phase coverage might tend to "average out" variations in G , but possibly not enough to justify treating $\hat{\sigma}_{oc}$ as an approximation to R . In any event, we argue that 1986 DA's large albedo relative to those of S NEAs strongly favors its identification with irons rather than with E chondrites, as follows.

If S NEAs are stony irons [a hypothesis defended by mineralogical interpretations of reflectance spectra for several large S MBAs (5)] and 1986 DA is E chondritic, then we would expect 1986 DA to be roughly 70 percent as bright as S NEAs with similar regolith properties. If S NEAs are ordinary chondritic and 1986 DA is E chondritic, we would expect 1986 DA to be about 50 percent brighter than "typical" S NEAs. However, 1986 DA is about three times more reflective than the average S NEA and about four to ten times more reflective than the three radar-detected S NEAs that are

Table 2. Asteroid radar cross sections σ_{oc} , diameters D , radar albedos $\hat{\sigma}_{oc}$ and SC/OC ratios. Albedos are calculated from the diameters and the radar cross sections listed here. All of the radar cross sections and SC/OC ratios were measured by the authors at Arecibo (24, 30) except for 1566 Icarus (31). For Icarus and 97 Klotho, no SC data were taken. Relative uncertainties in Arecibo estimates of σ_{oc} are ~ 15 percent. MBA albedos use Infrared Astronomy Satellite (IRAS) radiometric diameters (32). Fractional standard errors in MBA diameter estimates are typically ~ 5 percent. The relative uncertainty in MBA albedo estimates is probably ~ 20 percent. As discussed in (33, 34), radiometric diameters are normally based on either a "standard" or "nonstandard" thermal model, or some hybrid of these two kinds of models. All of the MBA diameters reported here are standard model values. For NEAs, we use the radiometric diameter (4, 34) corresponding to the thermal model providing the best match to the available VIS-IR observations (35). All of the NEA diameters are standard model results except for five objects, as follows. For 1685 Toro, neither thermal model provides an acceptable fit to the VIS-IR data, and we adopt the radar result (13). For 3757 (1982 XB), neither thermal model is judged preferable, and we adopt the mean of the standard and nonstandard model diameters (0.5 and 0.7 km, respectively). Nonstandard model diameters are used for 1580 Betulia, 2100 Ra-Shalom, and 3199 Nefertiti. For the NEAs in this table, nonstandard diameters average $\sim 50\%$ larger than standard model diameters.

Asteroid		Class	σ_{oc} (km ²)	D (km)	$\hat{\sigma}_{oc}$	μ_c (± 0.10)
No.	Name*					
<i>Mainbelt asteroids (MBAs)</i>						
1	CER	C	33000	913	0.050	0.04
2	PAL	C	21000	523	0.10	0.05
5	AST	S	2400	125	0.20	0.20
6	HEB	S	4300	192	0.15	0.00
7	IRI	S	5900	203	0.18	0.08
8	FLO	S	1500	141	0.096	0.16
9	MET	S	3500	203	0.11	0.18
12	VIC	S	2100	117	0.20	0.14
16	PSY	M	1400	264	0.26	0.14
19	FCR	C	3200	221	0.085	0.04
41	DAP	C	2900	182	0.11	0.13
80	SAP	S	650	82	0.12	0.25
97	KLO	M	1100	87	0.18	
139	JUE	C	1300	162	0.063	0.10
144	VIB	C	1800	146	0.11	0.18
356	LIG	C	1800	135	0.13	0.12
554	PER	C	1600	99	0.21	0.06
694	EKA	C	610	93	0.09	0.00
<i>Near-Earth asteroids (NEAs)</i>						
433	ERO	S	75	22	0.20	0.22
1036	GAN	S	75	38.5	0.064	0.18
1566	ICA	S	0.1	0.9	0.16	
1580	BET	C	3.9	7.4	0.09	0.16
1620	GEO	S	0.9	2.0	0.29	0.19
1627	IVA	S	7.5	8.1	0.15	0.21
1685	TOR	S	1.6	3.3	0.19	0.18
1862	APO	Q	0.2	1.5	0.11	0.33
1866	SIS	S	8	8.2	0.15	0.32
1915	QUE	S	0.02	0.5	0.10	0.27
2100	RAS	C	0.8	2.4	0.18	0.26
3199	NEF	S	1.2	2.2	0.32	0.47
3757	1982 XB	S	0.018	0.6	0.06	0.27
1986 DA	1986 DA	M	2.4	2.3	0.58	0.09

*Abbreviated name.

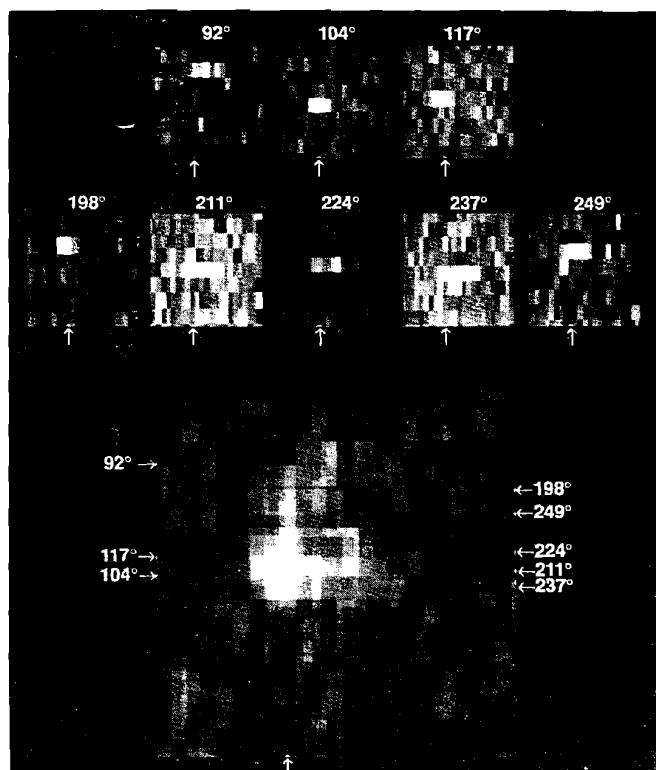


Fig. 3. Radar images of 1986 DA. The top two rows show images from the eight ranging runs taken at rotation phases indicated in the labels here and also in Fig. 1. Time delay, or range, increases from top to bottom and frequency increases from left to right. The resolution bins are defined by constant-delay planes normal to the line of sight and constant-frequency planes parallel to the plane that contains both the target's apparent spin vector and the radar. Brightness is proportional to OC echo power. Each square frame has a vertical extent of 5.0 km and a horizontal extent of 5.0 km/(cos δ). The vertical arrow at the bottom of each frame indicates the COM frequency, as determined from the hull estimation. That calculation yielded an offset, $f_c = -9.3$ Hz, of the COM frequency from the ephemeris prediction. That frequency-prediction error corresponds to a drift of $14 \mu\text{s}/\text{hour} = 2.1 \text{ km}/\text{hour}$ in the delay-prediction error; we compensated for that drift in constructing this figure. The large image at bottom is a superposition of the eight individual frames. Labels on the sides of that image indicate the range location of the peak echo in each of the individual frames.

less than one half its size. Therefore the hypothesis that 1986 DA is E chondritic seems untenable, independent of the S NEAs' meteoritic kinship.

On the other hand, if 1986 DA is a relatively regolith-free, iron-meteorite analog, then we can easily understand its albedo being much higher than typical S NEA albedos as long as S NEAs possess a significant regolith or are ordinary chondritic, or both. We reject the possibility that most S NEAs are regolith-free stony irons because most S NEA albedos are comparable to or smaller than those of so many objects that either are identified with intrinsically unreflective meteorites (C NEAs), or are likely to possess substantial regoliths (S MBAs), or both (C MBAs) (25).

Implications. The evidence that 1986 DA is metallic seems persuasive. How might this asteroid be "genetically" related to iron meteorites? Most irons are probably fragments of large cores of

parent asteroids that melted, differentiated, cooled, and solidified during the first billion years of the solar system and that subsequently suffered collisional disruption (26, 27). A meteorite's cosmic ray exposure (CRE) age marks the time when it was last shielded, by a meter or so of material, from energetic cosmic rays (26, 28). Most CRE ages reported for irons are between 200 and 1000 million years (My), comparable to the typical dynamical lifetime of an object in a Mars-crossing orbit, whereas only a few percent of those ages are as short as an Earth-crossing asteroid's typical lifetime of ~30 My (2). Any meteorites that originated as impact ejecta from 1986 DA may or may not have been launched before the asteroid evolved into an Earth-crossing orbit. The set of plausible CRE ages for such meteorites therefore includes virtually any value up to several billion years. Of course, 1986 DA might share the parentage of some meteorites or part of their dynamical history without ever

Table 3. Minerological and meteoritical associations of asteroid classes in Table 2. Meteorite analogs are from Lipschutz *et al.* (6). Typical densities and approximate abundances of metallics (native metals and metal sulfides) are from tables 2.1 and 4.1 of Dodd (36), table 24 of Buchwald (37), table 2 of Keil (38), and table 4.6 of Glass (39). High-iron (H) and low-iron (L)

chondrites are an order of magnitude more abundant than very low iron (LL) and enstatite (E) chondrites. The extremely rare Q asteroids might be analogous to ordinary chondrites (4). Abbreviations: wt, weight; and vol, volume.

Minerology	Possible meteorite analogs	Meteorite properties		
		Bulk density (g cm ⁻³)	Percent abundance of metallics	
			(wt)	(vol)
M asteroids				
Metal	Irons	7.6	97	97
Metal + enstatite	Enstatite chondrites	3.6	32	19
S asteroids				
Metal + olivine + pyroxene	Stony irons	4.9	50	30
Metal + olivine + pyroxene	Ordinary chondrites			
	H	3.6	24	12
	L	3.5	14	8
	LL	3.5	2	1
C asteroids				
Hydrated silicates + carbon-organics-opaques	Carbonaceous chondrites (CI1 and CM2)	2.6	11	6

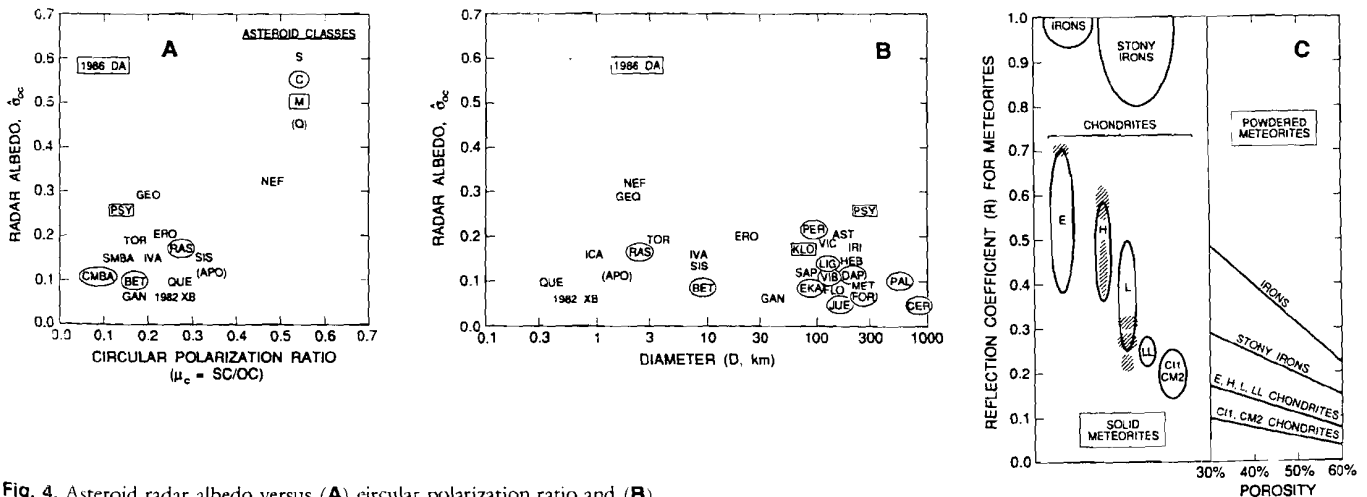


Fig. 4. Asteroid radar albedo versus (A) circular polarization ratio and (B) diameter. The values plotted in (A) and (B) are listed in Table 2. In (A) "SMBA" and "CMB" indicate mean values for seven S MBAs and nine C MBAs. (C) Reflection coefficient for meteorite types (Table 3). For dry, unconsolidated powders of meteoritic minerals, R depends primarily on bulk density d , and the curves show predictions of $R(d)$ based on the average of three empirically determined functions (24, 40) over the range of lunar-soil porosities (41). These curves probably are reliable to ± 25 percent. For solids,

small volume concentrations V of metal particles in a silicate matrix can increase R above the value for $V = 0$ by an amount that depends on the electrical properties of each phase, the metal particles' dimensions and packing geometry, and V . Here the oval fields show ranges of R expected for several meteorite types on the basis of laboratory investigations (42) of "loaded dielectrics." Cross-hatched fields show measurements of R for six meteorite specimens (22).

he
nd
nd
by
icy
in
ch
i.0
he
on
ris
14
for
a
nat
jal

having contributed any of its own ejecta to our meteorite sample. Gallium-germanium abundances in irons define groups that might share a common parent body, and ~40 percent of iron meteorites belong to two groups, IIIAB and IVA, each of whose CRE ages are narrowly clustered around a specific age (650 and 400 My, respectively) thought to correspond to major disruptions of these two groups' parent bodies (26, 29). Does 1986 DA share one of these groups' parentage? Or is it associated with one of the groups (such as IAB) whose CRE ages indicate involvement in at least four collisions between 100 and 1200 My ago? The many diverse possibilities seem indistinguishable at present. Analysis of samples returned from 1986 DA's surface by spacecraft would elucidate this asteroid's history and its meteoritic kinship.

REFERENCES AND NOTES

1. G. W. Wetherill, *Icarus* **76**, 1 (1988).
2. _____ and C. R. Chapman, in *Meteorites and the Early Solar System*, J. F. Kerridge and M. S. Matthews, Eds. (Univ. of Arizona, Tucson, 1988), pp. 35-67.
3. R. P. Binzel, T. Gehrels, M. S. Matthews, Eds., *Asteroids II* (Univ. of Arizona Press, Tucson, 1989).
4. L. A. McFadden, D. J. Tholen, G. J. Veeder, *ibid.*, pp. 442-467.
5. M. J. Gaffey, J. F. Bell, D. P. Cruikshank, *ibid.*, pp. 98-127.
6. M. E. Lipschutz, M. J. Gaffey, P. Pellas, *ibid.*, p. 740-777.
7. E. A. Cloutis, M. J. Gaffey, D. G. W. Smith, R. St J. Lambert, *J. Geophys. Res.* **95**, 281 (1990); D. F. Lupishko and I. N. Belskaya, *Icarus* **78**, 395 (1989).
8. E. F. Tedesco and J. C. Gradie, *Astron. J.* **93**, 738 (1987).
9. Among the several dozen classified NEAs, the S:C:M ratio is approximately 7:3:1 (4). Among the hundreds of classified MBAs, that ratio is approximately 7:5:1; see (5) and D. J. Tholen, thesis, University of Arizona, Tucson (1984). Asteroid taxonomic methods are reviewed by D. J. Tholen and M. A. Barucci, in (3), pp. 298-315.
10. M. Kizawa, *Int. Astron. Union Cir. 4181* (1986).
11. S. J. Ostro, in (3), pp. 192-212, and references therein.
12. _____ *et al.*, *Science* **248**, 1523 (1990).
13. S. J. Ostro, D. B. Campbell, I. I. Shapiro, *Astron. J.* **88**, 565 (1983).
14. S. J. Ostro *et al.*, *ibid.* **99**, 2012 (1990).
15. K. W. Zeigler, *Minor Planet Bull.* **17**, 1 (1990); W. Z. Wisniewski, *Icarus* **70**, 566 (1987).
16. G. Hahn, C.-I. Lagerkvist, M. Lindgren, M. Dahlgren, in *Asteroids, Comets, Meteors III*, C.-I. Lagerkvist, R. Rickman, B. A. Lindblad, M. Lindgren, Eds. (Uppsala University, Uppsala, 1990), pp. 95-98.
17. E. M. Shoemaker, R. F. Wolfe, C. S. Shoemaker, *Geol. Soc. Am. Spec. Pap.* **247**, 155 (1990); E. M. Shoemaker, J. G. Williams, E. F. Helin, R. F. Wolfe, in *Asteroids*, T. Gehrels, Ed. (Univ. of Arizona, Tucson, 1979), pp. 253-282.
18. S. J. Ostro, R. Connelly, L. Belkora, *Icarus* **73**, 15 (1988); S. J. Ostro, K. D. Rosema, R. F. Jurgens, *ibid.* **84**, 334 (1990). Uncertainties quoted for quantities related to the hull calculation are estimated standard errors.
19. M. A. Barucci and M. Fulchignoni, in *Asteroids, Comets, Meteors III*, C.-I. Lagerkvist, R. Rickman, B. A. Lindblad, M. Lindgren, Eds. (Uppsala University, Uppsala, 1990), pp. 101-105.
20. E. F. Tedesco, personal communication.
21. D. S. McKay, T. D. Swindle, R. Greenberg, in (3), pp. 617-642; K. R. Housen, L. L. Wilkening, C. R. Chapman, R. Greenberg, in *Asteroids*, T. Gehrels, Ed. (Univ. of Arizona, Tucson, 1979), pp. 601-627.
22. M. J. Campbell and J. Ulrichs, *J. Geophys. Res.* **74**, 5867 (1969).
23. R. A. Simpson, *Proc. IEEE Trans. Antenna Propag.* **AP-24**, 17 (1976).
24. S. J. Ostro, D. B. Campbell, I. I. Shapiro, *Science* **229**, 442 (1985).
25. S. J. Ostro *et al.*, in preparation.
26. E. R. D. Scott, in *Asteroids*, T. Gehrels, Ed. (Univ. of Arizona, Tucson, 1979), pp. 892-925.
27. _____ *et al.*, in (3), pp. 701-739.
28. J. T. Wasson, *Meteorites: Their Record of Early Solar System History* (Freeman, New York, 1985), pp. 58-61.
29. E. R. D. Scott and J. T. Wasson, *Rev. Geophys. Space Phys.* **13**, 527 (1975).
30. S. J. Ostro, D. B. Campbell, I. I. Shapiro, *Bull. Am. Astron. Soc.* **17**, 729 (1985).
31. R. M. Goldstein, *Science* **162**, 903 (1968).
32. E. F. Tedesco, in (3), pp. 1090-1150.
33. L. A. Lebofsky and J. R. Spencer, in (3), pp. 128-147; M. V. Sykes and R. L. Walker, *Science* **251**, 777 (1991).
34. G. J. Veeder *et al.*, *Astron. J.* **97**, 1211 (1989). Absolute uncertainties in NEA radiometric diameters are probably several tens of percent; relative uncertainties are probably somewhat smaller.
35. G. L. Veeder, personal communication.
36. R. T. Dodd, *Meteorites* (Cambridge Univ. Press, Cambridge, 1981).
37. V. F. Buchwald, *Handbook of Iron Meteorites* (Univ. of California Press, Berkeley, 1975), p. 86.
38. K. Keil, *J. Geophys. Res.* **73**, 6945 (1968).
39. B. P. Glass, *Introduction to Planetary Geology* (Cambridge Univ. Press, Cambridge, 1982).
40. J. B. Garvin, J. W. Head, G. H. Pettengill, S. H. Zisk, *J. Geophys. Res.* **90**, 6657 (1985); F. T. Ulaby *et al.*, *IEEE Trans. Geosci. Remote Sensing* **28**, 325 (1990).
41. W. D. Carrier III, J. K. Mitchell, A. Mahmood, *Proc. Lunar Sci. Conf.* **4**, 2-303 (1973).
42. J. M. Keilly, J. O. Stenoien, D. E. Isbell, *J. Appl. Phys.* **24**, 258 (1953); I. L. Nielson, *J. Phys. D: Appl. Phys.* **7**, 1549 (1974); G. H. Pettengill, P. G. Forness, D. Chapman, *J. Geophys. Res.* **93**, 14881 (1988).
43. We thank the staff of the Arecibo Observatory for assistance with the observations. Part of this research was conducted at the Jet Propulsion Laboratory, California Institute of Technology, under contract with the National Aeronautics and Space Administration (NASA). J.F.C. and I.I.S. were supported in part by NASA. Arecibo Observatory is part of the National Astronomy and Ionosphere Center, which is operated by Cornell University under a cooperative agreement with the National Science Foundation and with support from NASA.

14 March 1991; accepted 26 April 1991